

## Uses of $\alpha$ -Fe<sub>2</sub>O<sub>3</sub> and fly ash as solid adsorbents

J SHAKHAPURE, H VIJAYANAND, S BASAVARAJA,  
V HIREMATH<sup>†</sup> and A VENKATARAMAN\*

Department of Materials Science, Gulbarga University, Gulbarga 585 106, India

<sup>†</sup>Department of Chemistry, PDA Engineering College, Gulbarga 585 101, India

MS received 10 May 2005; revised 7 September 2005

**Abstract.** Solid adsorbents have shown great promise for control of particulate and non-particulate matter and as gas sensing devices in recent times. In the present study, adsorption of environmental toxic pollutant such as lead ions on solid adsorbents viz.  $\alpha$ -Fe<sub>2</sub>O<sub>3</sub> and fly ash, are reported. Considerable adsorption was observed on fly ash when compared to  $\alpha$ -Fe<sub>2</sub>O<sub>3</sub> surface. These studies are characterized by employing solid state and solution studies.

**Keywords.** Lead adsorption;  $\alpha$ -Fe<sub>2</sub>O<sub>3</sub>; fly ash; structure; morphology.

### 1. Introduction

Various chemical pollutants are released in high quantities into the atmosphere as a result of human activities, thereby generating environmental pollution. In order to monitor the pollution on a large scale, inexpensive, reliable and easy to use solid adsorbents/chemical sensors are needed (Gopel 1994; Yamazoe and Miura 1994; Sun *et al* 1995). Metal oxides, especially iron and manganese oxides, and organic materials, have high surface area and are dominant solid adsorbent materials, because of their capacities to adsorb heavy metals (Dong *et al* 2002).

$\alpha$ -Fe<sub>2</sub>O<sub>3</sub> is a conventional semiconductor material, which has been widely applied as active catalytic, magnetic, nonlinear optics and gas sensitive material (Ai *et al* 1994; Kandori *et al* 1995; Ocana *et al* 1995; Cannas *et al* 1998). These properties are due to the high surface area and porosity possessed by the  $\alpha$ -Fe<sub>2</sub>O<sub>3</sub> particles (Ying 1992; Huo *et al* 2000).  $\alpha$ -Fe<sub>2</sub>O<sub>3</sub> is commonly found in soils in some regions (Schulze 1989; Heshem and Watson 1998), and it can also be easily synthesized in the laboratory in a short time.

Fly ash is a coal product generated in particle sizes ranging between 150 nm and 120  $\mu$ m. It is abrasive and refractory in nature. Chemically, fly ash consists of silica to an extent of 55–70% followed by alumina, 10–18%, iron oxide, 6–20%, lime magnesia and alkalies varying between 1 and 5% each. Fly ash generally consists of elements like Cu, Ag, Pb, Cd, Fe, Mn, Ti, Na, Cl, Mo, S, P and Zn in different concentrations depending upon type of coal used (Pedlow 1978; Valkovic *et al* 1992; Karwas 1995). Less than half of the ash is used as a raw

material for concrete manufacturing and construction; the remaining being directly dumped as waste. Due to shortage of landfill sites and environmental regulations, new ways of utilizing fly ash are needed. Since fly ash consists of metal oxides and has high surface area and porosity, these features are expected to increase the adsorption sites on fly ash. Fly ash also consists of hollow spherical particles called cenospheres (Shigenato *et al* 1993), which has considerable importance in weight specific applications.

Lead is a metal that is emitted to air as small particles. In the past, automobiles were the major contributors of lead emissions to the atmosphere. Presently lead is found in considerable extent in paint, inks, water supply and distribution systems, pesticides, and fresh and processed food. Numerous studies have demonstrated that exposure to lead adversely affects human health. Lead has its most pronounced effect on the hemotopoietic (blood-forming), nervous and renal (kidney) systems, but may also harm the reproductive, endocrine, hepatic, cardiovascular, immunologic, and gastrointestinal systems.

Several processes have been used and developed over the years to remove metals dissolved in industrial waste waters through chemical precipitation, ion exchange, membrane filtration or adsorption. The latter has been studied for both mineral and organic materials. Silica gel and alumina show excellent adsorption behaviour. Presence of silanol groups on the surface of the silica gel and the vacant sites and porosity in the structure of the alumina and silica are mainly responsible for the adsorption behaviour (Michard *et al* 1996; Towle *et al* 1997; Tran *et al* 1999). Some of the other uses of iron oxide reported include, as an agent for making the halogen containing waste gases harmless (Yuji *et al* 2001), removal of phosphate from water (Okamoto *et al* 1996) and removal of oil from water (Onoda and Moriyama 1975). Dong *et al* (2001) reported

\*Author for correspondence (raman\_chem@rediffmail.com)

that Pb and Cd adsorption to the surface coating was dominated by Mn and Fe oxides. They also reported that metal oxides were more effective than organic material in adsorbing lead from water. In our earlier work, we have reported the understanding of the adsorption behaviour of  $\text{Ca}^{2+}$  ions on rubber- $\alpha\text{-Fe}_2\text{O}_3$  composite (Vijayanand *et al* 2002) and adsorption of lead on magnetic iron oxides and their complex composites (Lagashetty *et al* 2003a; Mallikarjuna and Venkataraman 2003).

This work is a continuation of our ongoing work on understanding the adsorption behaviour of heavy metals on magnetic and nonmagnetic metal oxides (Lagashetty and Venkataraman 2004; Govindraj *et al* 2005). The present work involves study of adsorption behaviour of lead ions on  $\alpha\text{-Fe}_2\text{O}_3$  and fly ash employing structural and morphological characterization. Solid-state adsorption studies are undertaken to understand the spectroscopic features and morphology of the adsorbate molecules. The bonding between the adsorbate and the adsorbent molecules is usually studied employing infrared spectroscopy and the structural features are understood from the X-ray diffraction (XRD) studies (Lagashetty *et al* 2003a; Mallikarjuna and Venkataraman 2003; Lagashetty and Venkataraman 2004; Govindraj *et al* 2005). The morphology study employing scanning electron micrograph (SEM) and energy dispersive X-ray microanalysis (EDX) techniques helps us to know the morphological changes of the adsorbent and the amount of adsorption (Lagashetty *et al* 2003b; Mallikarjuna and Venkataraman 2003; Lagashetty and Venkataraman 2004; Govindraj *et al* 2005), respectively. Upon adsorption even finer details about surface area can be understood from SEM studies.

## 2. Experimental

### 2.1 Materials and methods

Red oxide, fly ash, hydrochloric acid, liquor ammonia, lead acetate and double distilled water were used. All the chemicals used were of AR grade. Red oxide of grade IS-445 was purchased commercially. Fly ash was taken as supplied from the commercial firm (Gift sample from Shradha Building Materials, Valsad, Gujarat). The activation of  $\alpha\text{-Fe}_2\text{O}_3$  and fly ash was carried out employing wet ball milling and the procedure employed has been reported earlier (Venkataraman *et al* 2001). The static method reported in our earlier studies (Mallikarjuna and Venkataraman 2003) was employed for the adsorption study.

### 2.2 Purification of $\alpha\text{-Fe}_2\text{O}_3$

The purification of  $\alpha\text{-Fe}_2\text{O}_3$  from red oxide was carried out and reported in our earlier work (Havanoor *et al* 2003).

### 2.3 Preparation of columns

A glass column of equal length and diameter was taken. The bottom of the empty column was packed with glass wool for about 1 cm height. 1 g of  $\alpha\text{-Fe}_2\text{O}_3$ /fly ash was poured onto the column and packed uniformly by tapping the column.

### 2.4 Adsorption studies

To the above said columns, 50 ml of known concentration of lead acetate was poured and kept aside for adsorption for 12 h. The solution was then eluted and subjected to atomic absorption spectroscopy (AAS) for the determination of lead ions. The solid adsorbent was dried in air and was characterized by X-ray diffraction (XRD), infrared (IR), scanning electron micrograph (SEM), and energy dispersive X-ray microanalysis (EDX) techniques.

### 2.5 Characterization

The powder X-ray diffraction (XRD) patterns were collected from JEOL JDX-8030 X-ray diffractometer using  $\text{CuK}\alpha$  radiation and indexing were done by JCPDS files. The coupled SEM and energy dispersive X-ray microanalyses of the samples were obtained from JSM-840A scanning electron microscope. The infrared measurements were carried out using a Perkin Elmer FT-IR spectrometer in the range  $4000\text{--}400\text{ cm}^{-1}$ . The atomic absorption spectroscopy measurements were carried out using Smith-Hieftji 1000 model.

## 3. Results and discussion

### 3.1 Infrared (IR) studies

The adsorbents were investigated for the adsorption behaviour of lead on  $\alpha\text{-Fe}_2\text{O}_3$ /fly ash surfaces from infrared spectra. Various vibrational frequencies of lead adsorbed  $\alpha\text{-Fe}_2\text{O}_3$ /fly ash are given in table 1. The vibrational bands of pure  $\alpha\text{-Fe}_2\text{O}_3$  and pure fly ash are also given in table 1 for the sake of comparison. The bands below  $1000\text{ cm}^{-1}$  in table 1 for all samples are characteristic peaks for metal-oxygen vibrational frequencies. Some

**Table 1.** Vibrational frequencies of pure and adsorbed  $\alpha\text{-Fe}_2\text{O}_3$  and fly ash.

Sample	Observed peaks frequency ( $\text{cm}^{-1}$ )
$\alpha\text{-Fe}_2\text{O}_3$	3120, 1074, 550 and 456
Lead adsorbed $\alpha\text{-Fe}_2\text{O}_3$	1554, 1105, 1010, 540 and 445
Fly ash	3451, 1600, 1094, 560 and 474
Lead adsorbed fly ash	1560, 1230, 1120, 1065, 554 and 480

additional peaks were also observed in adsorbed samples when compared with the IR spectra of pure samples. These peaks are understood to be due to the presence of the vibrational modes of lead adsorption on the surface.

### 3.2 X-ray diffraction (XRD) studies

The X-ray diffraction patterns of the pure  $\alpha$ -Fe<sub>2</sub>O<sub>3</sub> and fly ash used in the present work, are shown in figures 1(a) and 3(a), respectively. In figure 1(a), all the peaks matched well with those reported for well crystallized  $\alpha$ -Fe<sub>2</sub>O<sub>3</sub> (JCPDS file No. 24-72), having rhombohedral structure. Figure 3(a) shows the XRD pattern of fly ash. Figures 2(a) and 4(a) show the XRD patterns of lead adsorbed  $\alpha$ -Fe<sub>2</sub>O<sub>3</sub> and fly ash, respectively. On careful observation of these figures, we notice the presence of some additional reflections along with those corresponding to pure  $\alpha$ -Fe<sub>2</sub>O<sub>3</sub> and fly ash. These additional peaks correspond to lead, which are adsorbed on the surface of the  $\alpha$ -Fe<sub>2</sub>O<sub>3</sub>/fly ash and are indexed on comparison with the JCPDS file No. 44-0872 for Pb. These XRD patterns thus confirm the adsorption of lead ions on the surface of the  $\alpha$ -Fe<sub>2</sub>O<sub>3</sub>/fly ash, respectively.

### 3.3 Energy dispersive X-ray microanalysis (EDX) studies

The EDX were carried out to know the presence of adsorbed lead on the  $\alpha$ -Fe<sub>2</sub>O<sub>3</sub> and fly ash surfaces. Figures 1(b) and 2(b) show EDX spectra of the pure and lead adsorbed  $\alpha$ -Fe<sub>2</sub>O<sub>3</sub>, respectively. Figures 3(b) and 4(b) show the EDX spectra of the fly ash and lead adsorbed fly ash.

On comparison of figure 2(b) with figure 1(b), figure 2(b) shows the presence of both Pb and Fe atoms. This EDX analysis confirms the fact that the  $\alpha$ -Fe<sub>2</sub>O<sub>3</sub> adsorbs a considerable amount of lead ions. Adsorption of lead on fly ash was also observed (figure 4b).

### 3.4 Scanning electron micrographic (SEM) studies

The surface morphologies of the pure and lead adsorbed  $\alpha$ -Fe<sub>2</sub>O<sub>3</sub> and fly ash are observed by scanning electron micrographic images as shown in figures 1(c) and 2(c) and 3(c) and 4(c), respectively. Figure 1(c) shows SEM image of as synthesized  $\alpha$ -Fe<sub>2</sub>O<sub>3</sub>. From this image one can see clearly that particles have various shapes and sizes in the range 100–300 nm. Also an important feature is that there is no aggregation of particles to form giant structures instead, all particles are individual. Figure 2(c)

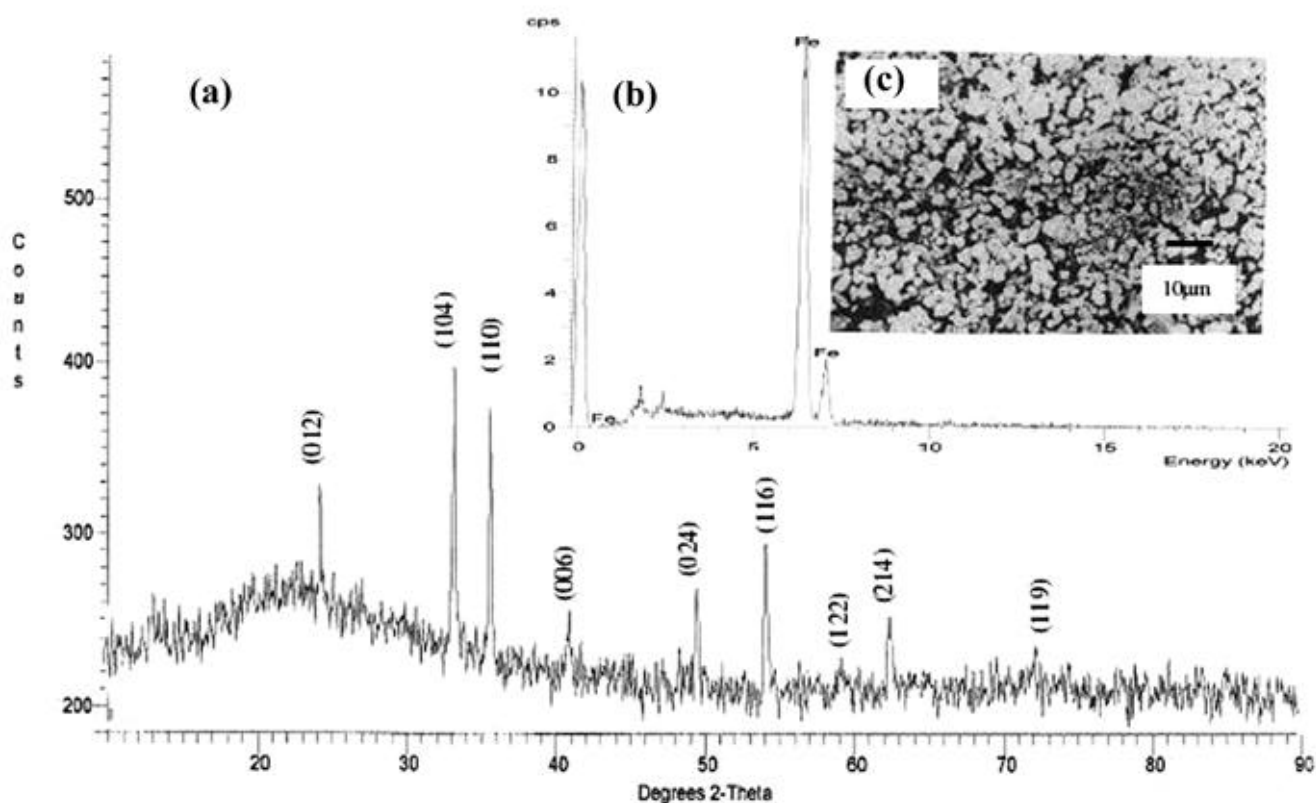


**Figure 1.** (a) XRD pattern of  $\alpha$ -Fe<sub>2</sub>O<sub>3</sub>, (b) EDX spectra of  $\alpha$ -Fe<sub>2</sub>O<sub>3</sub> and (c) SEM image of  $\alpha$ -Fe<sub>2</sub>O<sub>3</sub>.

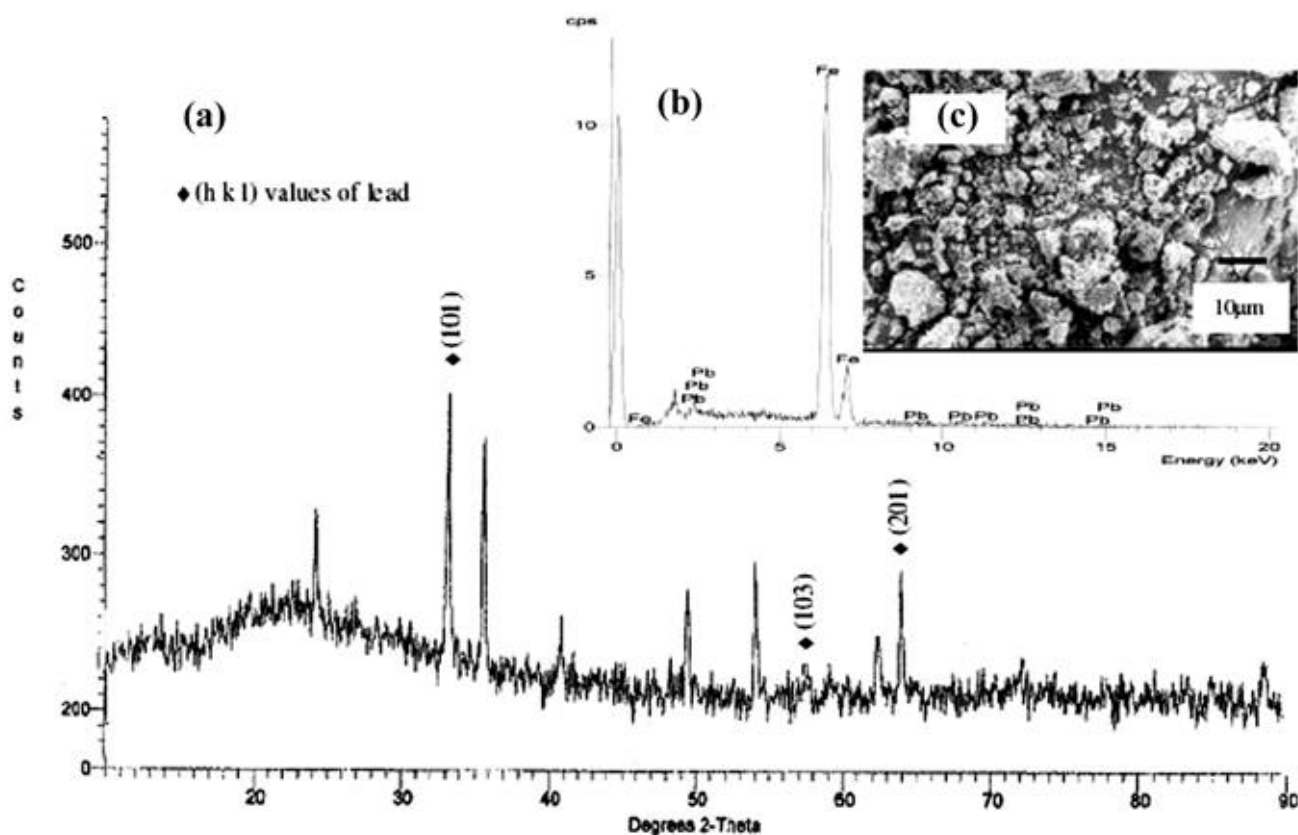
shows SEM image of lead adsorbed  $\alpha$ -Fe<sub>2</sub>O<sub>3</sub>. The image shows the close joint of  $\alpha$ -Fe<sub>2</sub>O<sub>3</sub> with lead adsorbed on it. Some agglomerates of particles are also observed. It may thus be understood that upon adsorption the individual  $\alpha$ -Fe<sub>2</sub>O<sub>3</sub> particles get closely jointed. The SEM image shows marginal changes in the morphology when compared with the understood  $\alpha$ -Fe<sub>2</sub>O<sub>3</sub> (figure 2(c)). The changes include formation of agglomerates and deposition of ultrafine particles possibly of lead. Similar changes in morphologies before and after adsorption of metals on other metal oxide surfaces were reported by us earlier (Lagashetty *et al* 2003a; Mallikarjuna and Venkataraman 2003; Lagashetty and Venkataraman 2004). Hence, it may be felt that understanding of changes in the surface morphology plays a role in adsorption process.

Figure 3(c) shows SEM image of pure fly ash. Some hollow tiny spherical particles are observed in the images and these tiny spheres are called cenospheres (Shigenato *et al* 1993) with diameters of the cenospheres in the range 300–600 nm. Some agglomerates of particles are also observed in the image. Figure 4(c) shows SEM image of the lead adsorbed fly ash. The morphology of the adsorbed fly ash has changed to some extent. This figure also shows the possible adsorption of ultrafine particles of lead on the surface of cenospheres of fly ash.

### 3.5 Atomic absorption spectroscopic (AAS) studies

AAS gives important information regarding the percentage of the metal present in a solution quantitatively and qualitatively. AAS was carried out for lead acetate (blank) solution and eluent solution (after passing through the columns in both the cases, i.e. for  $\alpha$ -Fe<sub>2</sub>O<sub>3</sub> and fly ash). The results are given in table 2. The eluent obtained after adsorption shows the decrease in the amount (26 and 46% on  $\alpha$ -Fe<sub>2</sub>O<sub>3</sub> and fly ash, respectively) of lead. This indicates that a considerable amount of lead ions get adsorbed on the surface of  $\alpha$ -Fe<sub>2</sub>O<sub>3</sub> and fly ash.

The possible mechanism of adsorption on  $\alpha$ -Fe<sub>2</sub>O<sub>3</sub> may be understood as the formation of outer sphere complex between the surface hydroxyl groups (chemisorbed water or adsorbed water) present on the surface of the adsorbent,  $\alpha$ -Fe<sub>2</sub>O<sub>3</sub>, and the adsorbate lead ions. Outer sphere complex is formed mainly from electrostatic interactions and contains more than one water molecules between the adsorbate and the adsorbent functional groups (Sposito 1989). In another case the formation of inner sphere complex (inner sphere formed via a ligand exchange reaction between adsorbent and adsorbate (Sposito 1989)) between the adsorbent (amorphous iron oxide) and adsorbate (arsenic (V)) is reported (Hsia *et al* 1992).



**Figure 2.** (a) XRD pattern of lead adsorbed  $\alpha$ -Fe<sub>2</sub>O<sub>3</sub>, (b) EDX spectra of lead adsorbed  $\alpha$ -Fe<sub>2</sub>O<sub>3</sub> and (c) SEM image of lead adsorbed  $\alpha$ -Fe<sub>2</sub>O<sub>3</sub>.

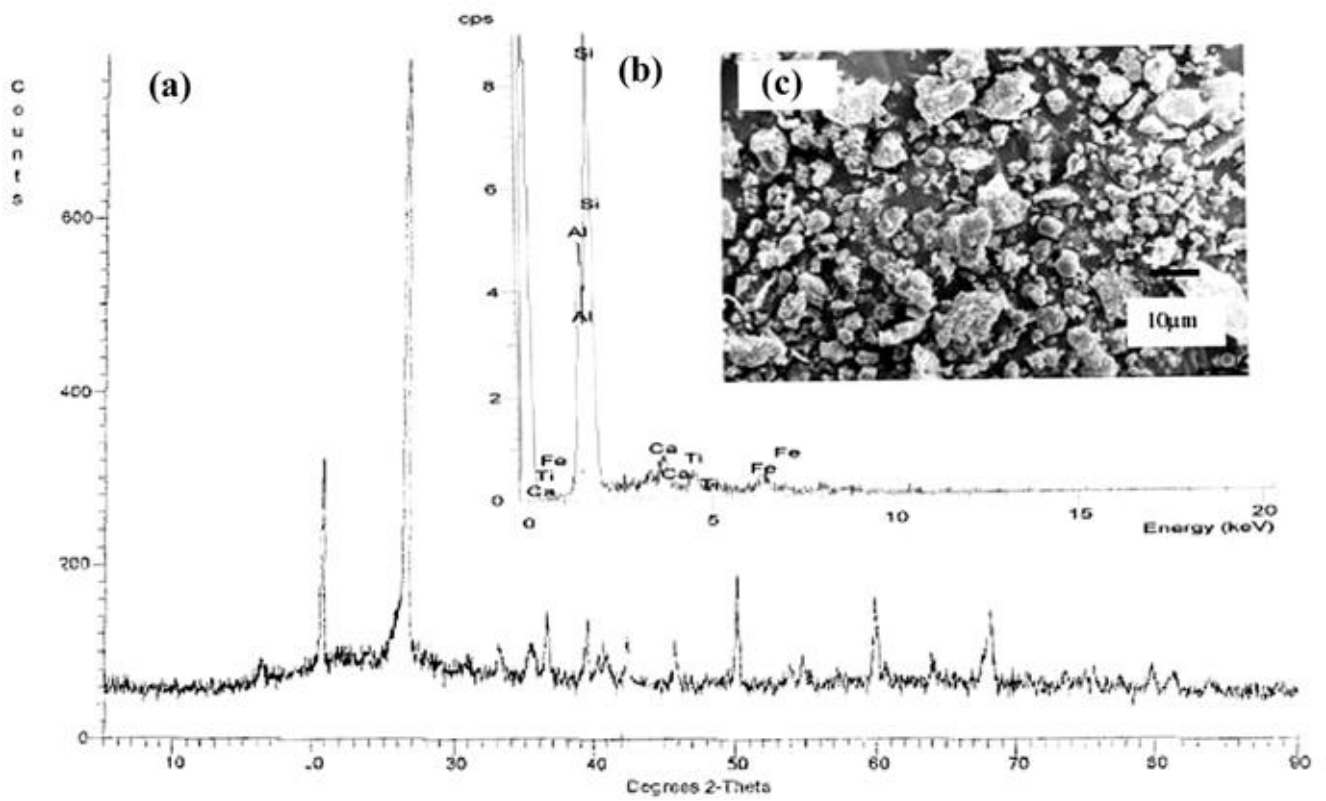


Figure 3. (a) XRD pattern of fly ash, (b) EDX spectra of fly ash and (c) SEM image of fly ash.

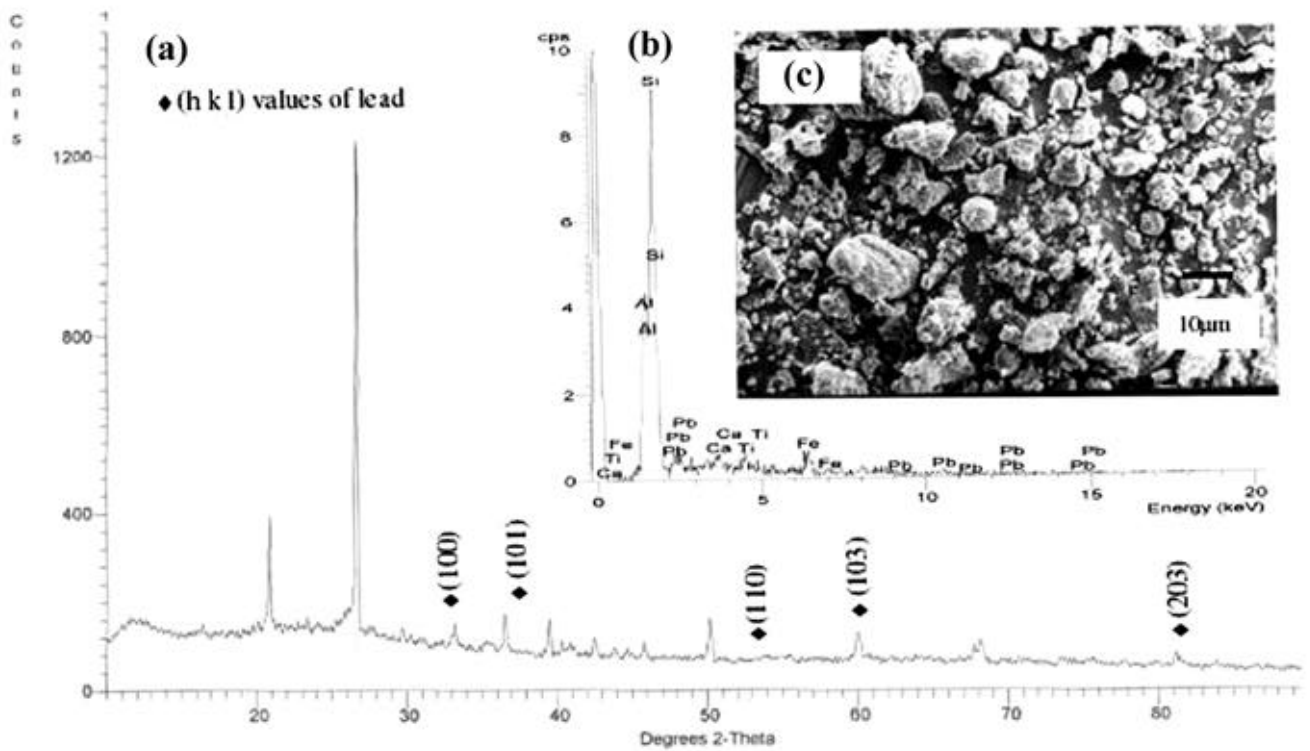


Figure 4. (a) XRD pattern of lead adsorbed fly ash, (b) EDX of lead adsorbed fly ash and (c) SEM image of lead adsorbed fly ash.

**Table 2.** Atomic absorption results.

Initial concentration of lead ions	18.58 mg	–
After passing through $\alpha$ -Fe <sub>2</sub> O <sub>3</sub>	13.67 mg	26.43% adsorption
After passing through fly ash	10.74 mg	42.2% adsorption

However, in the present study formation of outer sphere complex may be envisaged, as there occurs water of hydration on the surface of  $\alpha$ -Fe<sub>2</sub>O<sub>3</sub>. This is in concurrence with the XRD and IR result of  $\alpha$ -Fe<sub>2</sub>O<sub>3</sub>, shown in figures 2(a) and 2(c), respectively.

It is generally believed that the presence of defects, adatoms, porosity, or vacancies creates active sites and enhances the surface activity (Calatayud et al 2004). Fly ash consists of silica, alumina and iron oxides in high proportions. Fly ash contains silica (55–70%), alumina (10–18%) and iron oxide (6–20%) (Pedlow 1978; Valkovic et al 1992; Karwas 1995). Because of these oxides there would be silinol groups from silica and hydroxyl groups from alumina and iron oxides, which aid in bonding with adsorbate molecules. The adsorption will be further enhanced by the presence of metal atoms, vacant sites, defects, etc present in the surface of the fly ash (Michard et al 1996; Towle et al 1997; Tran et al 1999).

#### 4. Conclusions

Based on the studies carried out in the present investigation, following conclusions are made:

- (I) The results obtained from IR, XRD, SEM and EDX techniques supplement the adsorption of lead on  $\alpha$ -Fe<sub>2</sub>O<sub>3</sub> and fly ash surfaces.
- (II) The AAS results also collaborate the above results on adsorption.
- (III) Amongst the two solid adsorbents viz.  $\alpha$ -Fe<sub>2</sub>O<sub>3</sub> and fly ash, employed in the present study, fly ash shows higher adsorption due to the presence of metal oxides and vacant sites present on the surface of the fly ash.
- (IV) A detailed understanding about the quantitative aspects and the structural transformations is the future direction of our work.

#### Acknowledgements

One of the authors (SB) thanks the University Grants Commission (UGC) for financial assistance. Part of the work was presented at 16th AGM, MRSI, 2005, Pune.

#### References

- Ai X C, Fei H S and Yang Y Q 1994 *J. Lumin.* **61–62** 364  
 Calatayud M, Markovits A and Minot C 2004 *Catalysis Today* **89** 269  
 Cannas C, Gatteschi D, Musinu A, Piccaluga G and Sangregoria C 1998 *J. Phys. Chem.* **B102** 7721  
 Dong Deming, Li Yu and Hua Xiuyi 2001 *Microchem. J.* **70** 25  
 Dong Deming, Hua Xiuyi, Li Yu and Li Zhonghua 2002 *Environmental Pollution* **119** 317  
 Gopel W 1994 *Sensors Actuators* **B18–19** 1  
 Govindraj B, Vijayanand H and Venkataraman A 2005 *Synth. & React. Inorg. & Metal. Org. Chem.* (submitted)  
 Havanoor V V, Mallikarjuna N N, Lagashetty A and Venkataraman A 2003 *Asian J. Chem.* **15** 79  
 Heshem Abdel-Smad and Watson Philip R 1998 *Appl. Surface Sci.* **136** 46  
 Hsia T H, Lo S F and Lin C F 1992 *Chemosphere* **25** 1825  
 Huo L H et al 2000 *Chem. Mater.* **12** 790  
 Kandori K, Horil I and Yasukawa A 1995 *J. Mater. Sci.* **30** 2145  
 Karwas C P 1995 *J. Environ. Sci. Hlth.* **30** 1223  
 Lagashetty Arunkumar and Venkataraman A 2004 *Bull. Mater. Sci.* **27** 491  
 Lagashetty Arunkumar, Mallikarjuna N N and Venkataraman A 2003a *Indian J. Chem. Technol.* **10** 63  
 Lagashetty Arunkumar, Havanoor Vijayanand, Mallikarjuna N N and Venkataraman A 2003b *Asian J. Chem.* **15** 1500  
 Mallikarjuna N N and Venkataraman A 2003 *Talanta* **60** 139  
 Michard P, Guibal E, Vincent T and Cloirec J P Le 1996 *Microporous Mater.* **5** 309  
 Ocana M, Morales M P and Serna C T 1995 *J. Colloid Interface Sci.* **171** 85  
 Okamoto S, Kobuyashi K, Sato T and Hashioto K 1996 *Japan Kokai Tokyo*  
 Onoda I and Moriyama H 1975 *Japan Kokoi* **7** CODEN: JKXXXAF JP 50068982 19750609 Showa  
 Pedlow J W 1978 *Coal ash utilization fly ash, bottom ash and slag* (ed.) S Toreey (N J: Noyes Data Corporation) pp 353–362  
 Schulze D G 1989 *An introduction to soil clay mineralogy in Minerals in soil environments* (eds) J B Dixon and S B Weed (Madison, WI: Soil Science Society of America) 2nd ed., pp 379–438  
 Shigenato K, Haysi H and Mayuru K 1993 *J. Mater. Sci.* **28** 4581  
 Sposito G 1989 *The chemistry of soils* (New York: Oxford Univ. Press)  
 Sun Hong-Tao, Cantalini Carlo, Faccio Marco and Pelino Mario 1995 *Thin Solid Films* **269** 97  
 Towle S T, Barger J R, Brown G E Jr and Parks G A 1997 *J. Colloid Int. Sci.* **187** 62  
 Tran H H, Roddick F A and O'Donnell A J 1999 *Water Res.* **33** 2992  
 Valkovic O, Jaksic M, Caridi A, Cereda E, Haque A M I, Cherubini R, Maschini G and Menapace E 1992 *Nucl. Instrum. Meth. Phys. Res.* **B69** 479  
 Venkataraman A, Vijay A Hiremath, Date S K and Kulkarni S D 2001 *Bull. Mater. Sci.* **24** 617  
 Vijayanand H, Lagashetty A, Mallikarjuna N N and Venkataraman A 2002 *Asian J. Chem.* **15** 79  
 Yamazoe N and Miura N 1994 *Sensors Actuators* **B20** 95  
 Ying J Y 1992 *Mater. Lett.* **15** 180  
 Yuji H, Hitoshi A and Yoshio F 2001 *PCT Int. Appl.* **61** CODEN: PIXXD2 WO 0189666 A1 20011129